Identification of Human Hepatocellular Carcinoma-Related Biomarkers by Two-Dimensional Difference Gel Electrophoresis and Mass Spectrometry

ARTICLE *in* JOURNAL OF PROTEOME RESEARCH · NOVEMBER 2005

Impact Factor: 4.25 · DOI: 10.1021/pr0502018 · Source: PubMed

8 AUTHORS, INCLUDING:

Hsuan-Shu Lee
National Taiwan University
89 PUBLICATIONS **1,633** CITATIONS
SEE PROFILE

Guan-Tarn Huang
National Taiwan University
136 PUBLICATIONS **4,677** CITATIONS
SEE PROFILE

Lu-Ping Chow
National Taiwan University
60 PUBLICATIONS **1,228** CITATIONS
SEE PROFILE

research articles Journal of proteome research

Identification of Human Hepatocellular Carcinoma-Related Biomarkers by Two-Dimensional Difference Gel Electrophoresis and Mass Spectrometry

I-Neng Lee,[†] Chien-Hung Chen,[‡] Jin-Chuan Sheu*,[‡] Hsuan-Shu Lee,[‡] Guan-Tarn Huang,[‡] Chen-Yin Yu,[‡] Fung-Jou Lu,[†] and Lu-Ping Chow*,[†,§]

Graduate Institute of Biochemistry and Molecular Biology, College of Medicine, National Taiwan University, Taipei, Taiwan, Department of Internal Medicine, National Taiwan University Hospital and National Taiwan University College of Medicine, Taipei, Taiwan, and Department of Medical Genetics, National Taiwan University Hospital, Taipei, Taiwan

Received July 1, 2005

Hepatocellular carcinoma (HCC) is one of the leading causes of cancer-related death throughout the world. Although hepatitis B or C viral infections are main risk factors for HCC, the molecular mechanisms leading to HCC formation have not been clarified. To reduce the mortality and improve the effectiveness of therapy, it is important to search for changes in tumor-specific biomarkers whose function may involve in disease progression and which may be useful as potential therapeutic targets. In this study, we employed two-dimensional difference gel electrophoresis (2D-DIGE) combined with nano flow liquid chromatography tandem mass spectrometry (nanoLC−MS/MS) to investigate differentially expressed proteins in HCC. For each of eight HCC patients, Cy3-labeled proteins isolated from tumor tissue were combined with Cy5-labeled proteins isolated from the surrounding nontumor tissue and separated by 2D gel electrophoresis along with a Cy2-labeled mixture of all tumor and nontumor samples as an internal standard. Thirty-four protein spots corresponding to 30 different proteins were identified by nanoLC−MS/MS as showing significant change (paired *t*-test, $p < 0.05$) in the level of expression between tumor and nontumor tissues. Sixteen proteins were up-regulated and 14 were down-regulated in HCC; they seem to play important roles in a variety of pathways including glycolysis, fatty acid transport and trafficking, amino acid metabolism, iron and xenobiotic metabolism, ethanol metabolism, cell cycle regulation, cytoskeleton, and stress. A remarkable finding is the up-regulation of 14-3-3γ protein in HCC. 14-3-3 isoforms had been linked to carcinogenesis because they are involved in various cellular processes such as cell cycle regulation, apoptosis, proliferation, and differentiation. In conclusion, 2D-DIGE is an efficient strategy that enables us to identify differentially expressed proteins in HCC. Identification of potential biomarkers, such as the pinpointing of 14-3-3γ in our findings, may provide further useful insights into the pathogenesis of HCC.

Keywords: hepatocellular carcinoma • 2-D DIGE • nanoLC−MS/MS • 14-3-3γ • proteomics

Introduction

Hepatocellular carcinoma (HCC) represents the fourth most common malignant tumor worldwide. The incidence of HCC is high in the countries of Southeast Asia and South Africa. In Taiwan, it has been the leading cause of cancer death since 1984. About 6000−8000 people died of this cancer every year in Taiwan.[1] Major risks related to HCC are hepatitis B (HBV) and/or hepatitis C (HCV) virus infections, aflatoxin B1 exposure, alcohol drinking, and genetic defects.[2−4] Recent studies also indicate that the incidence of HCC in the North America and Europe has increased substantially over the last two decades.[5] However, the molecular mechanisms leading to the initiation and progression of this disease are not well-known, because most HCC patients are diagnosed at an advanced stage. To improve survival, further investigations of disease progression markers and the mechanisms of hepatocarcinogenesis are urgent.

Over the past decade, there has been significant progress in the development of systematic approaches to the study of HCC at the transcription and translation level. Several studies have

* To whom correspondence should be addressed. Lu−Ping Chow, Ph.D., Graduate Institute of Biochemistry and Molecular Biology, College of Medicine, National Taiwan University No. 1, Sec. 1, Jen-Ai Road, Taipei 100, Taiwan. Tel: 886-2-23123456 ext. 8212. Fax: 886-2-23958814. E-mail: lupin@ha.mc.ntu.edu.tw. Jin-Chuan Sheu, M. D. Ph.D., Department of Internal Medicine, National Taiwan University Hospital, No. 7, Chung-Shan South Road, Taipei 100, Taiwan. Tel: 886-2-23123456 ext. 6579. Fax: 886-2-23819723. E-mail: sheuhcc@ha.mc.ntu.edu.tw.

[†] Graduate Institute of Biochemistry and Molecular Biology, College of Medicine, National Taiwan University.

[‡] Department of Internal Medicine, National Taiwan University Hospital and National Taiwan University College of Medicine.

[§] Department of Medical Genetics, National Taiwan University Hospital.

Published on Web 11/05/2005
10.1021/pr0502018 CCC: $30.25

Table 1. Clinical and Pathological Data of Patients[a]

pt no.	age	sex	AFP (ng/mL)	HBsAg	anti-HCV	tumor size (cm)	grade	cirrhosis
1	52	M	10785	+	−	12	2−3	−
2	86	M	<20	−	−	10	2−3	−
3	66	M	<20	−	+	7	2	+
4	74	F	340	+	−	7	2	+
5	67	F	<20	+	+	4.5	2	+
6	81	M	2487	+	−	14	1−2	−
7	71	M	<20	+	+	15	3−4	+
8	65	M	<20	−	−	11	2	−

[a] M, male; F, female; AFP, α-fetoprotein; HBsAg, hepatitis B surface antigen; Anti-HCV, antibody for hepatitis C virus.

used a cDNA microarray approach to identify unique gene expression patterns that are associated with HCC,[6−8] and it has yielded some potential HCC markers such as osteopontin.[9] Traditional two-dimensional polyacrylamide gel electrophoresis (2D-PAGE) is one of the most commonly used proteomic approaches. Some earlier proteomic HCC studies used 2D-PAGE/post-staining and mass spectrometry to study differentially expressed proteins in cell lines,[10,11] and liver tumor tissues.[12−14] Among these, alterations of aldehyde dehydrogenase isozymes may be closely correlated to HCC, and lamin B1 was identified as a marker for cirrhosis.[12,13] Despite the fact that many HCC-associated proteins have been identified using this approach, most of them have not been confirmed due to a lack of appropriate antibodies.

Two-dimensional difference gel electrophoresis (2D-DIGE) is a modification of traditional 2D technology in which multiple protein samples can be pre-labeled with different fluorescence dyes, mix together and run on the same IEF gel and SDS-PAGE.[15−17] 2D-DIGE also introduces a pooled internal standard experimental design and co-detection technology, and therefore can overcome some disadvantages of traditional 2D. Recently, the 2D-DIGE approach has been successfully used to identify potential biomarkers of various cancers, such as colon cancer, esophageal carcinoma and breast cancer.[18−20]

In this study, we apply 2D-DIGE minimal labeling together with nano flow liquid chromatography tandem mass spectrometry (nanoLC−MS/MS) to detect differentially expressed proteins in HCC. Identification of these differentially expressed proteins may provide possible markers in liver carcinogenesis. Further investigation of these candidate markers using functional assays and careful study of many patients with proper statistical analysis may lead to markers that can be used clinically or alternatively may provide insight into the mechanisms of HCC progression.

Materials and Methods

Patients. A total of 8 HCC patients who had received surgical resectioning in National Taiwan University Hospital were enrolled. Primary HCC tissues and adjacent nontumor liver tissue from surgical specimens were frozen immediately after surgery and stored at −135 °C until use. The diagnosis of HCC was confirmed by pathological examination. The clinicopathological characteristics of the eight patients are shown in Table 1.

Protein Extraction. For each sample, the liver tissue was ground in a mortar filled with liquid nitrogen and precipitated with 10% TCA/acetone. The resultant precipitate was suspended in sample buffer (7 M urea, 2 M thiourea, 4% CHAPS, 10 mM Tris, 5 mM magnesium acetate, pH 8.0) and solubilized by sonication on ice. The pH of protein extract was adjusted to pH 8.5 by adding 50 mM NaOH, and protein concentration was determined using a 2D Quant kit (Amersham Biosciences, Uppsala, Sweden).

Cy-Dye Labeling. For DIGE minimal labeling, 50 μg of protein sample was mixed with 400 pmol CyDye (Amersham Biosciences) by vortexing and incubated on ice in the dark for 30 min. Proteins extracted from HCC tumor tissues and nontumor tissues were labeled with Cy3 and Cy5, respectively, then mixed with Cy2-labeled internal pooled standard and run on the same gel. The internal pooled standard sample was prepared by pooling 50 μg of protein from each of the 8 HCC tumor tissue samples together with similar samples from the 8 nontumor tissues prior to Cy2 labeling in the same manner as above. In all three cases the labeled sample was then quenched by the addition of 1 μL 10 mM lysine (Sigma-Aldrich, St. Louis, MO) followed by incubation on ice for a further 10 min.

Protein Separation by 2-DE. The quenched Cy3- and Cy5-labeled samples for each patient were then combined with the quenched Cy2-labeled pool internal standard. The total proteins (150 μg) were mixed and denatured in 2D sample buffer (8 M urea, 2% CHAPS, 2% IPG 3−10 buffer, 60 mM DTT), and then rehydrated with Immobiline DryStrip pH 3−10, 24 cm (Amersham Biosciences) in strip holder for the first-dimension isoelectric focusing (IEF). IEF was performed using Ettan IPGphor II horizontal electrophoresis system (Amersham Biosciences). The electrophoresis condition was set at 20 °C rehydration 10 h, step 1: 500 V 1 h, step 2: 1000 V 1 h, step 3: 8000 V 8 h. After IEF, the IPG strips were equilibrated and applied to the second dimension 12.5% SDS-PAGE using an Ettan Daltsix (Amersham Biosciences) electrophoresis system. For preparative purposes, IEF/SDS-PAGE was performed using 1 mg of internal pooled standard proteins, and the gel was stained with Coomassie blue (Amersham Biosciences).

Image Acquisition and Analysis. The Cy-dye labeled gels were visualized using a Typhoon 9410 imager (Amersham Biosciences). Excitation and emission wavelengths were chosen specifically for each of the dyes according to manufacturer's recommendations. Images were preprocessed to remove areas extraneous to those of interest using ImageQuant V5.2 (Amersham Biosciences). Intra-gel analysis was performed using DeCyder DIA (Difference In-gel Analysis) v5.0 (Amersham Biosciences). Inter-gel matching and statistical analysis were performed using DeCyder BVA (Biological Variance Analysis) v5.0 (Amersham Biosciences). The estimated number of spots for each co-detection procedure was set to 2500. The DeCyder DIA program uses a normal distribution model to determine the differentially expressed spots. The threshold was set to 2 standard deviations based on an assumption that 95% protein spots are not expected to be differentially expressed. Each protein in the individual sample is represented in the pooled standard, thus a comparison between the test samples and the identical protein in the standard can be used to generate a ratio of relative expression.

In-Gel Digestion. Proteins of interest were manually excised from a Commassie stained preparative gel and then destained with 50 mM ammonium bicarbonate/50% acetonitrile for 30 min to remove Coomassie blue staining, and dried in a SpeedVac concentrator as described previously.[21] The protein was digested with 10 μL sequencing grade trypsin (0.1 mg/mL; Promega, Madison, WI) in 50 mM ammonium bicarbonate

overnight at 37 °C. The resulting peptides were extracted from gel pieces with 1% trifluoroacetic acid by sonication, and then re-extracted with 0.1% trifluoroacetic acid/60% acetonitrile. The collected peptides were dried and reconstituted in 20 μL 5% acetonitrile/0.1% formic acid before mass spectrometry analysis.

LC−MS/MS Analysis. Nano-LC was performed using Ultimate nano high-performance liquid chromatography pump system (LC Packings, Amsterdam, Netherlands) and FAMOS autosampler (Dionex, Mountain View, CA). The trypsin-digested sample (5 μL) was injected via a sample loop (using 0.1% formic acid in water as carrier solvent) onto a 5 mm μ-Precolumn/Trap column (LC Packings). The sample was washed with 0.1% formic acid for 5 min on the Trap column before being switched onto a 15 cm × 75 μm Nano Series Standard Column (packed with C18 PepMap 100, 3 μm, 100 Å) (LC Packings) equilibrated with 95% mobile phase A (5% acetonitrile containing 0.1% formic acid) and 5% mobile phase B (80% acetonitrile containing 0.1% formic acid), at a flow rate of 200 nL/min. Five minutes after the sample was loaded, the proportion of mobile phase B was increased linearly to 40% over 50 min and then stepped to 90% within 5 min and maintained at this level for 15 min (wash phase). The column was then reequilibrated for 10 min with 95% mobile phase A/5% mobile phase B. The column effluent was continuously directed into a QSTAR XL mass spectrometer (Applied Biosystems, Foster city, CA) fitted with a nano-ESI source, and the spectra were acquired. Mass spectrometer conditions were calibrated using a purified renin fragment obtained from Applied Biosystems.

Protein Identification. Protein identification was performed using MASCOT software (www.matrixscience.com), and all tandem mass spectra were searched against the Swiss-Prot or NCBI nonredundant database. The following search parameters were used: trypsin was used as the cutting enzyme, mass tolerance for monoisotopic peptide window was set to ± 2 Da, the MS/MS tolerance window was set to ± 0.5 Da, one missed cleavage was allowed, and carbamidomethyl and oxidized methionine were chosen as fixed and variable modifications, respectively. Candidate sequences were identified from the database on the basis of intact peptide masses, and the complete or partial spectra expected to result from the fragmentation of these candidate peptides were generated and compared with the experimental spectrum.

Western Blotting of 14-3-3γ. 25 μg of tissue proteins were separated by 12.5% SDS-PAGE and transferred onto poly-(vinylidene difluoride) (PVDF) membrane (Millipore, Billerica, MA), which was then blocked for 1 h at 25 °C with 1% skimmed milk. 14-3-3γ was detected by incubation overnight at 4 °C with an anti-human 14-3-3γ polyclonal antibody (Santa Cruz Biotechnology Inc., Santa Cruz, CA). β-actin signal was detected by a mouse monoclonal anti-human β-actin antibody (Sigma-Aldrich) and used as an internal control. Protein signals were detected with Western Lightning Chemiluminescence Reagents (PerkinElmer Ltd., Boston, MA).

Statistical Analysis. Expression levels of 14-3-3γ in paired tumor and nontumor tissues were quantified by analyzing the band intensities of the Western blot with TotalLab software (Nonlinear Dynamics Ltd, Newcastle upon Tyne, UK). The statistical differences in 14-3-3γ expression levels between tumor and corresponding nontumor tissues were analyzed by the Student's paired *t*-test. p value < 0.05 was considered as significant.

Table 2. Experimental Design for 2D-DIGE Comparison of 8 HCCs and Their Adjacent Nontumor Tissues[a,b]

gel no.	Cy2	Cy3	Cy5
1	pooled std	tumor	nontumor
2	pooled std	tumor	nontumor
3	pooled std	tumor	nontumor
4	pooled std	nontumor	tumor
5	pooled std	nontumor	tumor
6	pooled std	tumor	nontumor
7	pooled std	nontumor	tumor
8	pooled std	nontumor	tumor

[a] Cy, cyanine dye; Std, standard. [b] The pooled standard consisting of an aliquot of all 16 samples used (8 tumors and 8 nontumors).

Results and Discussion

2D-DIGE Minimal Labeling. 2D-PAGE combined with post-staining has been proved to be an effective approach for the identification of tumor biomarkers. Recently, 2D-DIGE shows advantages over traditional 2D-PAGE in several aspects, including multiple pre-labeling of samples, introduced of a pooled internal standard, co-detection and wider dynamic range. When applied to analyze changes of protein expression level between large cohorts, it is able to save time and reduce the errors caused by gel-gel variation, and this allows easy data integration. In this study, protein profiles from eight HCC tumor tissues and their adjacent nontumor tissues were analyzed by 2D-DIGE technology followed by protein identification using nanoLC−MS/MS. As shown in Table 2, protein extracts were pre-labeled with either Cy3 or Cy5 fluorescent dyes, and then each case's Cy3/Cy5-labeled sample pair was co-mixed with a Cy2-labeled pooled standard sample containing an equal mixture of all 16 samples before running all three dye-labeled samples together on the same gel. We also adopted a dye swapping strategy to avoid dye labeling-bias, therefore, the Cy3 and Cy5 dyes were interchangeable.

A pseudocolor map of superimposed DIGE images is presented in Figure 1A, and Cy3 (tumor), Cy5 (nontumor), and Cy2 (pooled standard) spot maps of case 6 are shown in Figure 1B. For each case, the Cy3, Cy5, and Cy2 images were imported to DeCyder DIA (difference in-gel analysis) module to detect differentially expressed protein spot features in each gel. The Cy2 image increases the quality and reproducibility of 2D gel analysis by allowing local spot normalization and by providing reference spots for further gel-to-gel matching. The 2 S.D. (standard deviation) model was set as the threshold to define the spots that differ in their volumes between tumor and nontumor. The 2 S.D. cutoff indicates a volume ratio (tumor/nontumor) cutoff of 2 standard deviation based on the raw data set. In a normally distributed data set 95% of data points fall within this value. For detection of a significant change in expression level, we set threshold of 2 S.D. to ensure that volume ratio changes are unlikely to have occurred by chance.

The DIA result of each identified case is diagramed in Figure 2. DIA is only allowed for single pairwise comparisons and cannot be used to analyze the data generated by all gels for group statistical analysis. The threshold value (2 model S.D.) and number of differentially expressed spots are list in Table 3. To identify differentially expressed protein spots across these eight gels, the results from the intra-gel comparison (8 DIA files) were then imported into the BVA module of DeCyder software. The Cy2 image of case 6 was selected as the master, and the other 7 internal standard images were matched sequentially to it.

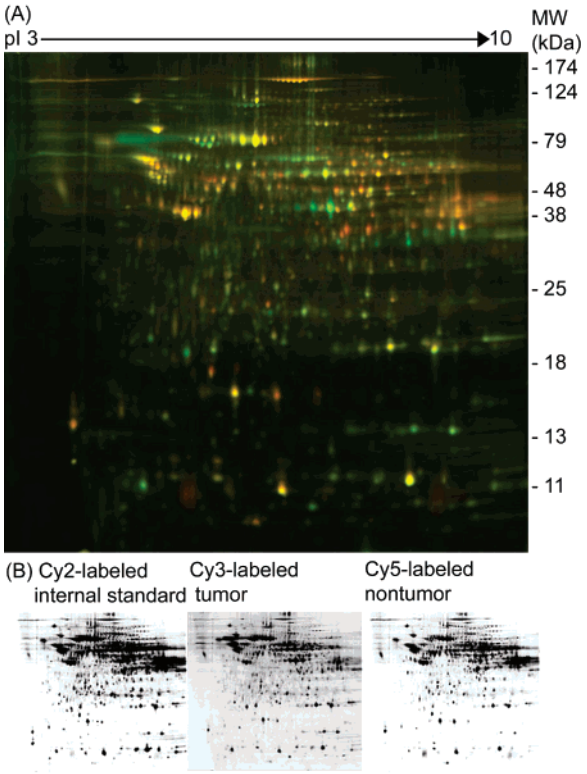

Figure 1. 2D-DIGE analysis of HCC case 6 using a pooled internal standard. Tumor proteins were labeled with Cy3 (green), nontumor proteins were labeled with Cy5 (red) and an aliquot of internal pooled standard lysates were labeled with Cy2. IEF was performed on 24 cm IPG strips, pH 3−10, and proteins were further separated by SDS-PAGE (12.5%) in 2D. (A) Image overlays of Cy3- and Cy5-labeled proteins. (B) Three separated Cy-dye images from pooled internal standard, tumor, and nontumor samples.

Table 3. Result of Difference In-Gel Analysis (DIA) of 8 HCC Cases

case 1	case 2	case 3
threshold value:2.85 decreased: 47 increased: 152 similar: 2091	threshold value:3.54 decreased: 69 increased: 91 similar: 2191	threshold value:2.68 decreased: 129 increased: 77 similar: 2155
case 4	**case 5**	**case 6**
threshold value:2.95 decreased: 71 increased: 47 similar: 2119	threshold value:2.65 decreased: 41 increased: 37 similar: 2198	threshold value:2.51 decreased: 120 increased: 34 similar: 2224
case 7	**case 8**	
threshold value:1.82 decreased: 88 increased: 92 similar: 2271	threshold value:3.51 decreased: 65 increased: 64 similar: 2110	

Identification of Differentially Expressed Proteins between HCC Tumors and Their Adjacent Nontumor Tissues by Mass Spectrometry. We performed Student's paired *t*-test ($p < 0.05$) to filter the protein spots that differentially expressed between tumor and nontumor groups. To identify these differentially expressed proteins, the spots of interest were excised from the preparative gel, and in-gel trypsin digestion and nanoLC−MS/MS analysis were performed for protein identification. At least two peptides of experimental MS/MS data matched to the theoretical candidate protein internal sequence was considered as a successful identification. We totally identified 34 differentially expressed protein spots that were matched to the output of the BVA analysis. The positions of those differentially expressed spots in the preparative 2D gel are shown in Figure 3. The results of protein identification are listed in Table 4 and Table 5 including spot number, protein name, score, sequence coverage, theoretical M*r*/p*I*, *p* value and predict function.

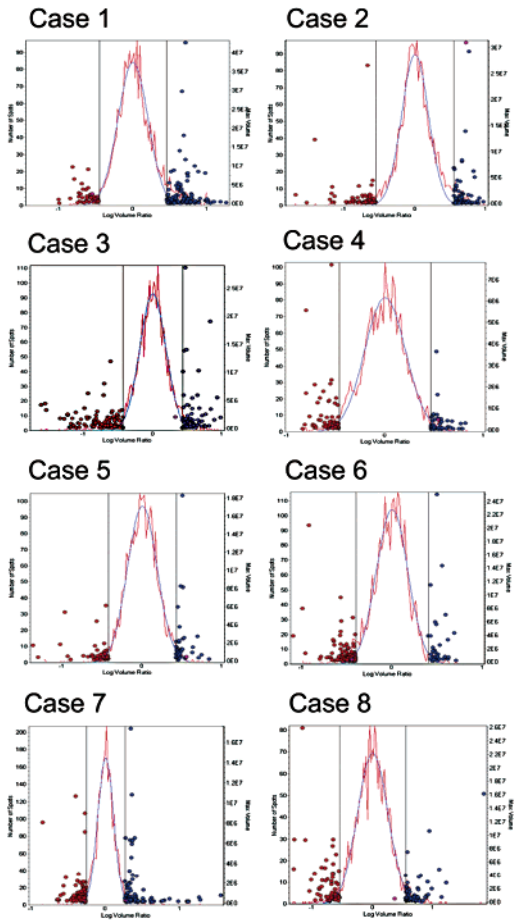

Figure 2. Determining the differentially expressed proteins in 8 gels. The histograms were generated by DeCyder DIA software, plotting spot frequency (left *y*-axis) against log volume ratio (*x*-axis), and a normal distribution model (red line) was fitted to the main peak of the frequency histogram. A 2 S.D. (standard deviation) model was set as threshold. The threshold values are represented by vertical black lines in the histogram, and the differentially expressed spot features are shown as blue spots and red spots. The number of increased expressed spot, decreased expressed spot, similar expressed spot, and threshold value of each case were shown in Table 3.

Of the sixteen identified up-regulated proteins in HCC (Table 4), four were categorized as cytoskeletal proteins, two as heat shock proteins and chaperones, four as metabolic enzymes, two participated in antioxidative system and redox mechanism, one involved in cell cycle regulation, and three proteins had unknown function by bioinformatics ontology. Triosephosphate isomerase is a glycolytic pathway enzyme and related to energy production. Up-regulation of triosephosphate isomerase has been reported in a previous HCV-related HCC proteomic

Table 4. Up-Regulated Proteins in Human HCC Tissues

spot no.	name	score	coverage (%)	MW (kD)/p*I*	*p* value[a]	function
7	triosephosphate isomerase	409	31	26.52/6.51	0.00051	glycometabolism
9	TPMsk3 (tropomyosin fragment)	251	22	28.79/4.72	0.0029	cytoskeleton
10	14−3−3 protein gamma	73	16	28.15/4.8	0.00075	cell cycle
11	heat shock protein 27	187	28	22.77/5.98	0.0044	stress
17−20	heat shock protein 70 kDa	569	27	70.85/5.37	0.0022	stress
16	class IVb beta tubulin	458	33	49.72/4.82	0.0094	cytoskeleton
15	actin gamma 1	219	23	41.77/5.31	0.0064	cytoskeleton
30	methionine adenosyltransferase	112	6	37.54/6.9	0.014	amino acid metabolism
1	thioredoxin	51	12	11.60/4.82	0.11	redox mechanism
34	profilin, chain A	164	34	14.84/8.46	0.043	actin polymerization
5	peptidylprolyl isomerase	98	10	18.00/7.68	0.029	protein metabolism
29	3-hydroxysteroid dehydrogenase	355	24	37.07/6.71	0.025	steroid metabolism
12	glutathione S-transferase omega 1	182	20	23.33/6.75	0.0008	antioxidative system
35	AX887972 NID	197	44	18.06/7.68	0.0012	unknown
36	AF110731 NID	268	28	22.01/8.85	0.0014	unknown
25	BC008837 NID	277	18	36.00/7.12	0.014	unknown

[a] *p* value was generated by Decyder BVA analysis.

Table 5. Down-Regulated Proteins in Human HCC Tissues

spot no.	name	score	coverage (%)	MW (kD)/p*I*	*p* value[a]	function
2	cathepsin D, chain A	43	8	10.67/5.65	0.00027	aspartic protease
4	fatty acid-binding protein	392	84	14.12/6.6	0.01	fatty acid metabolism
8	carbonic anhydrase II	309	31	28.75/6.63	0.001	Acid−base balance
13	cathepsin D, chain B	247	26	26.23/5.31	0.021	aspartyl protease
14	nicotinamide *N*-methyltransferase	196	20	29.56/5.56	0.0056	xenobiotic metabolism
6	ferritin light chain	41	4	20.01/5.51	0.025	iron-buffering
16	actin-related protein 2/3 complex subunit 5	115	22	16.18/5.47	0.0025	cytoskeleton
28	fructose-1,6-biphosphatase	179	16	36.66/6.6	0.0048	glycometabolism
27	alcohol dehydrogenase	153	13	36.42/6.34	0.028	ethanol catabolism
26	acyl-CoA dehydrogenase	261	12	44.27/8.13	0.028	fatty acid metabolism
33	glutamate dehydrogenase	441	14	61.36/7.66	0.0014	nitrogen metabolism
31	fructose-bisphosphate aldolase	145	7	39.44/8.0	0.058	glycometabolism
21	aminoacylase	72	5	45.86/5.77	0.022	detoxification enzyme
32	haptoglobin precursor	146	11	38.43/6.13	0.015	immune response
5	AX969436 NID	92	16	14.81/6.26	0.009	unknown

[a] *p* value was generated by Decyder BVA analysis.

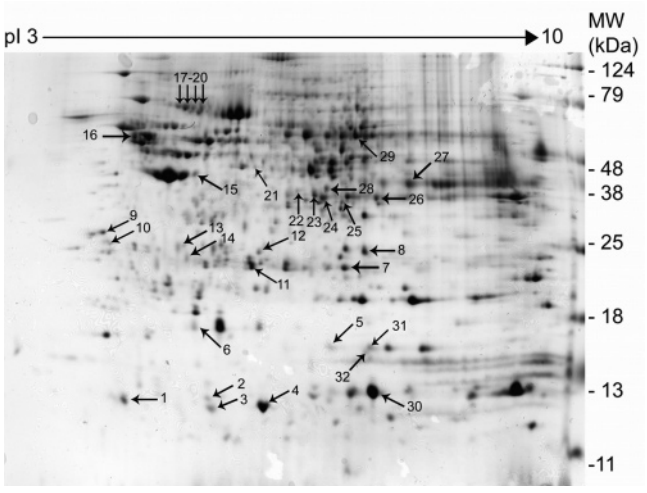

Figure 3. Representative 2D image of the preparative gel. One milligram of internal pool standard proteins was used to perform IEF using Immobiline DryStrip pH 3−10, 24 cm and then separated with a 12.5% SDS-PAGE. The gel was post-staining with Coomassie blue. Arrows indicate differentially expressed proteins, and they were excised from the gel and subjected to in-gel digestion and nanoLC−MS/MS analysis.

study.[22] Heat shock proteins overexpressed in HCC are a common event in hepatic carcinogenesis, and at least five-members of this family (HSP90, HSP70, HSC71, HSP60, HSP27) have been reported in previous studies.[13,22,23] Cytoskeletons such as β-tubulin and actin γ-1 have also been shown to be increased in HCC. Profilins regulate actin polymerization through binding and subsequently sequestering the actin monomer.[24] In fact, some chemotherapeutic agents use the antitumor effects caused by inhibition of tubulin polymerization.[25,26] Methionine metabolism and the methylation cycle are known to be altered in several liver disorders. Methionine adenosyltransferase (MAT) is responsible for the conversion of methionine into S-adenosylmethionine (AdoMet). AdoMet synthesis and utilization is impaired in conditions such as liver cirrhosis and cancer. Up-regulation of methionine adenosyltransferase is thus consistent with other gene expression studies, and one study indicated that the MAT II β subunit provides a proliferative advantage in human hepatoma cell lines and that this effect could be mediated through its interaction with MAT II α2 and the downregulation of AdoMet levels.[27] However, Liang et al. found that the methionine adenosyltransferase was down-regulated in poorly differentiated HCC.[28] The discrepancy between these results has not yet been clarified. Elevated serum level of thioredoxin has been noted in patients with HCC.[29] Peptidylproplyl isomerase up-regulates β-catenin by inhibiting its interaction with APC, and has been found to be overexpressed in HCC.[13,30] 3-hydroxysteroid dehydrogenases could inactivate steroid hormones in the liver, however, its role in hepatocarcinogenesis needs further clarification. Glutathione-S-transferases (GSTs) are a

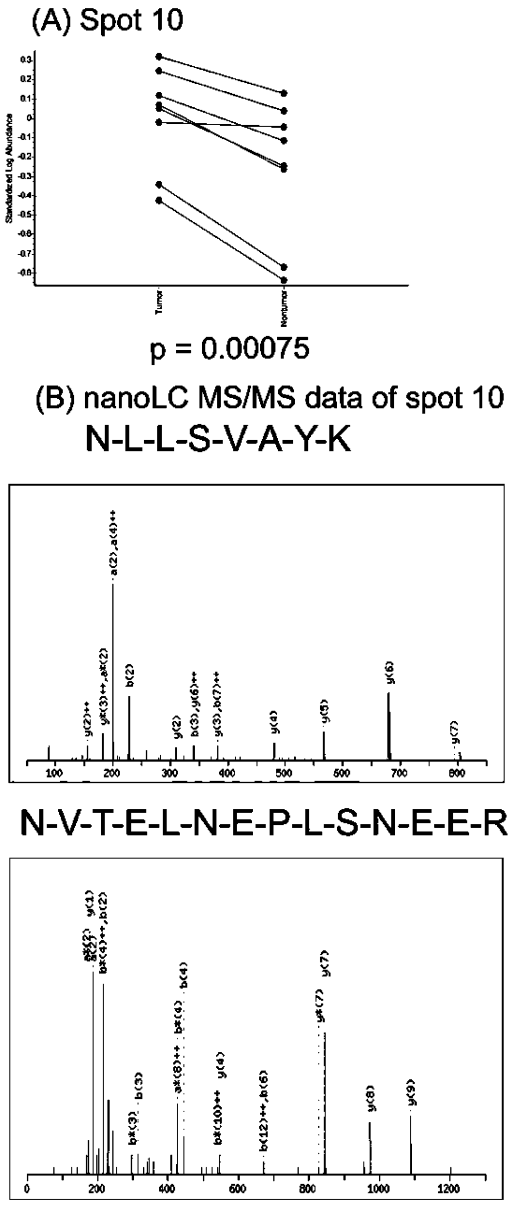

Figure 4. (A) Graphical representation of the distribution across the 8 gels of spot 10 expression level in tumor tissues and their corresponding nontumor tissues. The *p* value derived from paired *t*-test is shown at the bottom. (B) Representative spectrum of nanoLC−MS/MS, showing MS/MS fragmentation patterns of two peptides from spot 10, 14-3-3γ protein.

family of phase II detoxification enzymes that catalyze the conjugation of glutathione to a wide variety of xenobiotic compounds. GSTs are known to be involved in carcinogen metabolism, and thus might be involved in the hepatocarcinogenesis.

A total of 14 proteins with decreased expression levels in HCC tissues were successfully identified (Table 5). Most of these proteins had been reported previously to be down-regulated in HCC, and they might reflect the de-differentiated phenotype of the hepatocytes. Decreased expression of fatty acid-binding protein has been identified by two previous studies of HCC.[13,24] Park et al. used 2D gel to show tissue ferritin light chain, an iron-storage protein, was either severely suppressed or reduced to undetectable levels in HCC.[14] Cathepsin D was shown to be

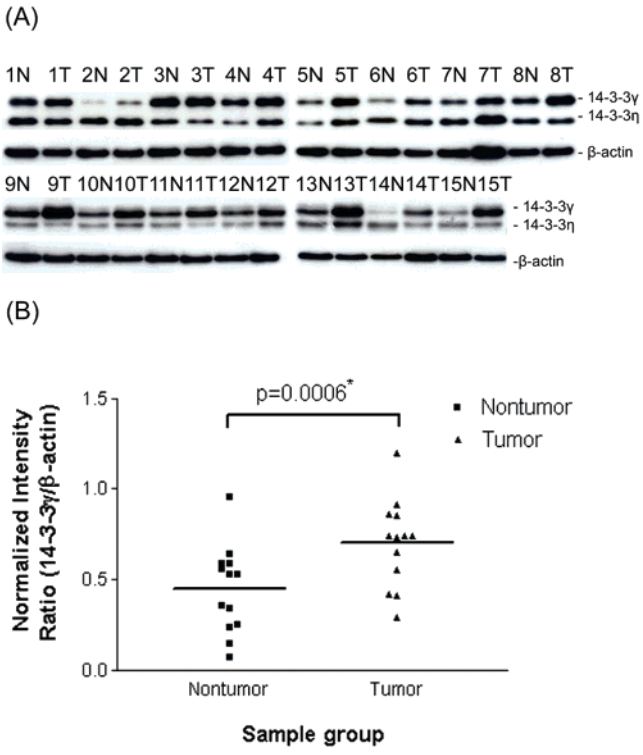

Figure 5. (A) Western blotting analysis of 14-3-3γ in the 8 HCC DIGE cases (1−8) and also 7 additional HCC cases (9−15). 14-3-3γ polyclonal antibody has partial cross reactivity with 14-3-3η. (B) Differences in expression were analyzed by the Student's paired *t*-test ($p < 0.05$). The expression levels of 14-3-3γ were up-regulated significantly in tumor tissues.

down-regulated in two proteomic hepatoma cell line-based studies after transfection with a nuclear factor construct or in cells with different metastasis potentials.[31,32] The actin-related protein 2/3 (Arp2/3) complex is known to play an important role in the control of actin polymerization, and the maintenance of the cell shape.[33] Decreased expression of the Arp2/3 complex had been reported in gastric cancer,[34] but not in HCC. Aminoacylase hydrolyses act on a variety of N-acylated amino acids to generate free amino acids and may be involved in the synthesis of hippurate that is formed during detoxification of aromatic compounds.[35] Decreased expression of this enzyme has also been reported in renal cell carcinoma and small cell lung cancer cell lines.[36,37]

In brief, the identified differentially expressed proteins between HCC tumor tissues and nontumor tissues are related to many biological pathways in the hepatocyte, including glycolysis, fatty acid transport and trafficking, amino acid metabolism, iron and xenobiotic metabolism, ethanol metabolism, cell cycle regulation, ATP synthesis, and stress. Although the majority of the proteins identified in this study have been reported in previous 2D-based HCC studies, the results suggest that 2D-DIGE is compatible with traditional 2D post-stained methods and overcomes some disadvantages as described above.

Validation of 14-3-3γ Expression by Western Blotting. From the list of differentially proteins, one of them is of special interest. Figure 4A shows the up-regulation of spot 10 in HCC tumor tissues by BVA analysis. Spot 10 was subsequently identified as 14-3-3γ by nanoLC−MS/MS analysis with a MASCOT score of 73 (Figure 4B). We focused on this protein

because it was related to cell cycle regulation. To validated the 2D-DIGE data, changes in the expression levels of 14-3-3γ were measured by immunoblot analysis in 15 pair of HCC tissues (8 DIGE HCC cases and 7 additional HCC cases, Figure 5A). Semiquantitative analysis of the expression of 14-3-3γ normalized to the amount of β-actin present in the samples showed that HCC malignant tissues has an increased ratio of expression of 14-3-3γ compared with matched nonmalignant tissues ($p = 0.0006$, Figure 5B). Deregulation of 14-3-3 proteins may determine whether a cell to undergo proliferation or apoptosis.[38] 14-3-3γ protein is a member of a multifunctional protein family comprising seven mammalian isoforms (β, γ, ϵ, η, σ, τ, and ζ). It has been reported that 14-3-3 proteins regulate numerous cellular circuits that are implicated in cancer development.[39] The mitosis promoting phosphatase, cdc25C, is a target of both the DNA replication and DNA damage checkpoint pathways. These two pathways regulate cdc25C function in part, by promoting the association of cdc25C with 14-3-3 proteins, which results in the retention of cdc25C in the cytoplasm. Two 14-3-3 family members, 14-3-3ϵ and 14-3-3γ, specifically form a complex with cdc25C and induce premature chromatin condensation (PCC) in U-2OS cells.[40] Iwata et al. reported that hypermethylation of CpG islands of the 14-3-3σ gene was detected in 89% of the HCC tissues, and loss of protein expression was detected by immunohistochemical staining.[41] 14-3-3σ inactivation by epigenetic silencing has also been seen in a number of other tumor types, such as prostate cancer, lung cancer, neuroendocrine tumors, and breast cancer.[42−45] The pathophysiological importance of changes in 14-3-3 protein isoform expression, regulation and localization in hepatocacinogenesis remains to be determined.

Conclusions

We have used 2D-DIGE minimal labeling to analyze the proteome of HCC tumor tissues and their surrounding nontumor parts. We identified at least 34 protein spots corresponding to 30 different proteins with differentially expressed levels in HCC, and they played important roles in a variety of pathways. The 2D liver protein maps presented in this study could be used as reference database in future HCC proteomic studies. It is expected that our results will help an understanding of the pathogenesis mechanism of HCC and provide information that will help the search for therapy and treatments for HCC.

Acknowledgment. The authors thank the financial support of (1) Grant NSC 92-2314-B-002-143 from the National Science Council, Taiwan, (2) Promotion of Research-oriented university program from the Ministry of Education of the Taiwan, and (3) grants from Liver Disease Prevention & Treatment Research Foundation, Taiwan in this project.

References

(1) Chen, D. S. Hepatitis B virus infection, its sequelae, and prevention in Taiwan. In *Neoplasms of the liver*; Okuda, K.; Ishak, K. G., Eds. Springer-Verlag: Tokyo, 1987; pp 71−80.
(2) Ogunbiyi, J. O. Hepatocellular carcinoma in the developing world. *Semin. Oncol.* **2001**, *28*(2), 179−187.
(3) Lopez, L. J.; Marrero, J. A. Hepatocellular carcinoma. *Curr. Opin. Gastroenterol.* **2004**, *20*(3), 248−253.
(4) Thorgeirsson, S. S.; Grisham, J. W. Molecular pathogenesis of human hepatocellular carcinoma. *Nat. Genet.* **2002**, *31*(4), 339−346.
(5) El-Serag, H. B., Hepatocellular carcinoma: recent trends in the United States. *Gastroenterology* **2004**, *127*, (5 Suppl 1), S27−34.
(6) Okabe, H.; Satoh, S.; Kato, T.; Kitahara, O.; Yanagawa, R.; Yamaoka, Y.; Tsunoda, T.; Furukawa, Y.; Nakamura, Y. Genome-wide analysis of gene expression in human hepatocellular carcinomas using cDNA microarray: identification of genes involved in viral carcinogenesis and tumor progression. *Cancer Res.* **2001**, *61* (5), 2129−2137.
(7) Chen, X.; Cheung, S. T.; So, S.; Fan, S. T.; Barry, C.; Higgins, J.; Lai, K. M.; Ji, J.; Dudoit, S.; Ng, I. O.; Van De Rijn, M.; Botstein, D.; Brown, P. O. Gene expression patterns in human liver cancers. *Mol. Biol. Cell.* **2002**, *13* (6), 1929−1939.
(8) Smith, M. W.; Yue, Z. N.; Geiss, G. K.; Sadovnikova, N. Y.; Carter, V. S.; Boix, L.; Lazaro, C. A.; Rosenberg, G. B.; Bumgarner, R. E.; Fausto, N.; Bruix, J.; Katze, M. G. Identification of novel tumor markers in hepatitis C virus-associated hepatocellular carcinoma. *Cancer Res.* **2003**, *63* (4), 859−864.
(9) Ye, Q. H.; Qin, L. X.; Forgues, M.; He, P.; Kim, J. W.; Peng, A. C.; Simon, R.; Li, Y.; Robles, A. I.; Chen, Y.; Ma, Z. C.; Wu, Z. Q.; Ye, S. L.; Liu, Y. K.; Tang, Z. Y.; Wang, X. W. Predicting hepatitis B virus-positive metastatic hepatocellular carcinomas using gene expression profiling and supervised machine learning. *Nat. Med.* **2003**, *9* (4), 416−423.
(10) Wirth, P. J.; Hoang, T. N.; Benjamin, T. Micropreparative immobilized pH gradient two-dimensional electrophoresis in combination with protein microsequencing for the analysis of human liver proteins. *Electrophoresis* **1995**, *16* (10), 1946−1960.
(11) Seow, T. K.; Ong, S. E.; Liang, R. C.; Ren, E. C.; Chan, L.; Ou, K.; Chung, M. C. Two-dimensional electrophoresis map of the human hepatocellular carcinoma cell line, HCC-M, and identification of the separated proteins by mass spectrometry. *Electrophoresis* **2000**, *21* (9), 1787−1813.
(12) Park, K. S.; Cho, S. Y.; Kim, H.; Paik, Y. K., Proteomic alterations of the variants of human aldehyde dehydrogenase isozymes correlate with hepatocellular carcinoma. *Int. J. Cancer* **2002**, *97*(2), 261−265.
(13) Lim, S. O.; Park, S. J.; Kim, W.; Park, S. G.; Kim, H. J.; Kim, Y. I.; Sohn, T. S.; Noh, J. H.; Jung, G. Proteome analysis of hepatocellular carcinoma. *Biochem. Biophys. Res. Commun.* **2002**, *291* (4), 1031−1037.
(14) Park, K. S.; Kim, H.; Kim, N. G.; Cho, S. Y.; Choi, K. H.; Seong, J. K.; Paik, Y. K. Proteomic analysis and molecular characterization of tissue ferritin light chain in hepatocellular carcinoma. *Hepatology* **2002**, *35* (6), 1459−1466.
(15) Knowles, M. R.; Cervino, S.; Skynner, H. A.; Hunt, S. P.; de Felipe, C.; Salim, K.; Meneses-Lorente, G.; McAllister, G.; Guest, P. C. Multiplex proteomic analysis by two-dimensional differential in-gel electrophoresis. *Proteomics* **2003**, *3* (7), 1162−1171.
(16) Shaw, J.; Rowlinson, R.; Nickson, J.; Stone, T.; Sweet, A.; Williams, K.; Tonge, R. Evaluation of saturation labeling two-dimensional difference gel electrophoresis fluorescent dyes. *Proteomics* **2003**, *3* (7), 1181−1195.
(17) Van den Bergh, G.; Arckens, L. Fluorescent two-dimensional difference gel electrophoresis unveils the potential of gel-based proteomics. *Curr. Opin. Biotechnol.* **2004**, *15* (1), 38−43.
(18) Friedman, D. B.; Hill, S.; Keller, J. W.; Merchant, N. B.; Levy, S. E.; Coffey, R. J.; Caprioli, R. M. Proteome analysis of human colon cancer by two-dimensional difference gel electrophoresis and mass spectrometry. *Proteomics* **2004**, *4* (3), 793−811.
(19) Zhou, G.; Li, H.; DeCamp, D.; Chen, S.; Shu, H.; Gong, Y.; Flaig, M.; Gillespie, J. W.; Hu, N.; Taylor, P. R.; Emmert-Buck, M. R.; Liotta, L. A.; Petricoin, E. F., 3rd; Zhao, Y. 2D differential in-gel electrophoresis for the identification of esophageal scans cell cancer-specific protein markers. *Mol. Cell. Proteomics* **2002**, *1* (2), 117−124.
(20) Somiari, R. I.; Sullivan, A.; Russell, S.; Somiari, S.; Hu, H.; Jordan, R.; George, A.; Katenhusen, R.; Buchowiecka, A.; Arciero, C.; Brzeski, H.; Hooke, J.; Shriver, C. High-throughput proteomic analysis of human infiltrating ductal carcinoma of the breast. *Proteomics* **2003**, *3* (10), 1863−1873.
(21) Moritz, R. L.; Eddes, J. S.; Reid, G. E.; Simpson, R. J. S-pyridylethylation of intact polyacrylamide gels and in situ digestion of electrophoretically separated proteins: a rapid mass spectrometric method for identifying cysteine-containing peptides. *Electrophoresis* **1996**, *17* (5), 907−917.
(22) Takashima, M.; Kuramitsu, Y.; Yokoyama, Y.; Iizuka, N.; Toda, T.; Sakaida, I.; Okita, K.; Oka, M.; Nakamura, K. Proteomic profiling of heat shock protein 70 family members as biomarkers for hepatitis C virus-related hepatocellular carcinoma. *Proteomics* **2003**, *3* (12), 2487−2493.

(23) Kim, W.; Oe Lim, S.; Kim, J. S.; Ryu, Y. H.; Byeon, J. Y.; Kim, H. J.; Kim, Y. I.; Heo, J. S.; Park, Y. M.; Jung, G. Comparison of proteome between hepatitis B virus- and hepatitis C virus-associated hepatocellular carcinoma. *Clin. Cancer Res.* **2003**, *9* (15), 5493−5500.
(24) Witke, W.; Podtelejnikov, A. V.; Di Nardo, A.; Sutherland, J. D.; Gurniak, C. B.; Dotti, C.; Mann, M. In mouse brain profilin I and profilin II associate with regulators of the endocytic pathway and actin assembly. *Embo J.* **1998**, *17* (4), 967−976.
(25) Li, J. N.; Song, D. Q.; Lin, Y. H.; Hu, Q. Y.; Yin, L.; Bekesi, G.; Holland, J. F.; Jiang, J. D. Inhibition of microtubule polymerization by 3-bromopropionylamino benzoylurea (JIMB01), a new cancericidal tubulin ligand. *Biochem. Pharmacol.* **2003**, *65* (10), 1691−1699.
(26) Ohno, T.; Kawano, K.; Sasaki, A.; Aramaki, M.; Tahara, K.; Etoh, T.; Kitano, S. Antitumor and antivascular effects of AC-7700, a combretastatin A-4 derivative, against rat liver cancer. *Int. J. Clin. Oncol.* **2002**, *7* (3), 171−176.
(27) Martinez-Chantar, M. L.; Garcia-Trevijano, E. R.; Latasa, M. U.; Martin-Duce, A.; Fortes, P.; Caballeria, J.; Avila, M. A.; Mato, J. M. Methionine adenosyltransferase II beta subunit gene expression provides a proliferative advantage in human hepatoma. *Gastroenterology* **2003**, *124* (4), 940−948.
(28) Liang, C. R.; Leow, C. K.; Neo, J. C.; Tan, G. S.; Lo, S. L.; Lim, J. W.; Seow, T. K.; Lai, P. B.; Chung, M. C. Proteome analysis of human hepatocellular carcinoma tissues by two-dimensional difference gel electrophoresis and mass spectrometry. *Proteomics* **2005**, *5* (8), 2258−2271.
(29) Miyazaki, K.; Noda, N.; Okada, S.; Hagiwara, Y.; Miyata, M.; Sakurabayashi, I.; Yamaguchi, N.; Sugimura, T.; Terada, M.; Wakasugi, H. Elevated serum level of thioredoxin in patients with hepatocellular carcinoma. *Biotherapy* **1998**, *11* (4), 277−288.
(30) Pang, R.; Yuen, J.; Yuen, M. F.; Lai, C. L.; Lee, T. K.; Man, K.; Poon, R. T.; Fan, S. T.; Wong, C. M.; Ng, I. O.; Kwong, Y. L.; Tse, E. PIN1 overexpression and beta-catenin gene mutations are distinct oncogenic events in human hepatocellular carcinoma. *Oncogene* **2004**, *23* (23), 4182−4186.
(31) Yuan, Q.; An, J.; Liu, D. G.; Sun, L.; Ge, Y. Z.; Huang, Y. L.; Xu, G. J.; Zhao, F. K. Proteomic analysis of differential protein expression in a human hepatoma revertant cell line by using an improved two-dimensional electrophoresis procedure combined with matrix assisted laser desorption/ionization-time-of-flight-mass spectrometry. *Electrophoresis* **2004**, *25* (7−8), 1160−1168.
(32) Ding, S. J.; Li, Y.; Shao, X. X.; Zhou, H.; Zeng, R.; Tang, Z. Y.; Xia, Q. C. Proteome analysis of hepatocellular carcinoma cell strains, MHCC97−H and MHCC97-L, with different metastasis potentials. *Proteomics* **2004**, *4*(4), 982−994.
(33) Welch, M. D., The world according to Arp: regulation of actin nucleation by the Arp2/3 complex. *Trends Cell. Biol.* **1999**, *9* (11), 423−427.
(34) Kaneda, A.; Kaminishi, M.; Sugimura, T.; Ushijima, T. Decreased expression of the seven ARP2/3 complex genes in human gastric cancers. *Cancer Lett.* **2004**, *212* (2), 203−210.
(35) Lindner, H.; Hopfner, S.; Tafler-Naumann, M.; Miko, M.; Konrad, L.; Rohm, K. H., The distribution of aminoacylase I among mammalian species and localization of the enzyme in porcine kidney. *Biochimie* **2000**, *82* (2), 129−137.
(36) Balabanov, S.; Zimmermann, U.; Protzel, C.; Scharf, C.; Klebingat, K. J.; Walther, R. Tumour-related enzyme alterations in the clear cell type of human renal cell carcinoma identified by two-dimensional gel electrophoresis. *Eur. J. Biochem.* **2001**, *268* (22), 5977−5980.
(37) Cook, R. M.; Franklin, W. A.; Moore, M. D.; Johnson, B. E.; Miller, Y. E. Mutational inactivation of aminoacylase-I in a small cell lung cancer cell line. *Genes Chromosomes Cancer* **1998**, *21* (4), 320−325.
(38) Vercoutter-Edouart, A. S.; Lemoine, J.; Le Bourhis, X.; Louis, H.; Boilly, B.; Nurcombe, V.; Revillion, F.; Peyrat, J. P.; Hondermarck, H. Proteomic analysis reveals that 14−3−3sigma is down-regulated in human breast cancer cells. *Cancer Res.* **2001**, *61* (1), 76−80.
(39) Hermeking, H. The 14-3-3 cancer connection. *Nat. Rev. Cancer* **2003**, *3* (12), 931−943.
(40) Dalal, S. N.; Yaffe, M. B.; DeCaprio, J. A. 14−3−3 family members act coordinately to regulate mitotic progression. *Cell Cycle* **2004**, *3* (5), 672−677.
(41) Iwata, N.; Yamamoto, H.; Sasaki, S.; Itoh, F.; Suzuki, H.; Kikuchi, T.; Kaneto, H.; Iku, S.; Ozeki, I.; Karino, Y.; Satoh, T.; Toyota, J.; Satoh, M.; Endo, T.; Imai, K. Frequent hypermethylation of CpG islands and loss of expression of the 14-3-3 sigma gene in human hepatocellular carcinoma. *Oncogene* **2000**, *19* (46), 5298−5302.
(42) Lodygin, D.; Diebold, J.; Hermeking, H. Prostate cancer is characterized by epigenetic silencing of 14-3-3 sigma expression. *Oncogene* **2004**, *23* (56), 9034−9041.
(43) Osada, H.; Tatematsu, Y.; Yatabe, Y.; Nakagawa, T.; Konishi, H.; Harano, T.; Tezel, E.; Takada, M.; Takahashi, T. Frequent and histological type-specific inactivation of 14-3-3 sigma in human lung cancers. *Oncogene* **2002**, *21* (15), 2418−2424.
(44) Yatabe, Y.; Osada, H.; Tatematsu, Y.; Mitsudomi, T.; Takahashi, T. Decreased expression of 14-3-3 sigma in neuroendocrine tumors is independent of origin and malignant potential. *Oncogene* **2002**, *21* (54), 8310−8319.
(45) Moreira, J. M.; Ohlsson, G.; Rank, F. E.; Celis, J. E. Down-regulation of the tumor suppressor protein 14−3−3sigma is a sporadic event in cancer of the breast. *Mol. Cell. Proteomics* **2005**, *4* (4), 555−569.

PR0502018